PHYSICAL REVIEW D **89,** 095028 (2014)

Present and future K and B meson mixing constraints on TeV scale left-right symmetry

Stefano Bertolini[*]
INFN, Sezione di Trieste, SISSA, via Bonomea 265, 34136 Trieste, Italy

Alessio Maiezza[†]
IFIC, Universitat de València-CSIC, Apt. Correus 22085, E-46071 València, Spain

Fabrizio Nesti[‡]
Ruđer Bošković Institute, Bijenička cesta 54, 10000, Zagreb, Croatia and Gran Sasso Science Institute, viale Crispi 7, I-67100 L'Aquila, Italy

(Received 3 April 2014; published 28 May 2014)

We revisit the $\Delta F = 2$ transitions in the K and $B_{d,s}$ neutral meson systems in the context of the minimal left-right symmetric model. We take into account, in addition to up-to-date phenomenological data, the contributions related to the renormalization of the flavor-changing neutral Higgs tree-level amplitude. These contributions were neglected in recent discussions, albeit formally needed in order to obtain a gauge-independent result. Their impact on the minimal LR model is crucial and twofold. First, the effects are relevant in B meson oscillations, for both CP conserving and CP violating observables, so that for the first time these imply constraints on the LR scenario which compete with those of the K sector (plagued by long-distance uncertainties). Second, they sizably contribute to the indirect kaon CP violation parameter ε. We discuss the bounds from B and K mesons in both cases of LR symmetry: generalized parity ($\mathcal{P}$) and charge conjugation ($\mathcal{C}$). In the case of $\mathcal{P}$, the interplay between the CP-violation parameters ε and ε' leads us to rule out the regime of very hierarchical bidoublet vacuum expectation values $v_2/v_1 < m_b/m_t \simeq 0.02$. In general, by minimizing the scalar field contribution up to the limit of the perturbative regime and by definite values of the relevant CP phases in the charged right-handed currents, we find that a right-handed gauge boson W_R as light as 3 TeV is allowed at the 95% C. L. This is well within the reach of direct detection at the next LHC run. If not discovered, within a decade the upgraded LHCb and Super B factories may reach an indirect sensitivity to a left-right scale of 8 TeV.

DOI: 10.1103/PhysRevD.89.095028 PACS numbers: 12.60.Cn, 14.40.Df, 14.40.Nd

I. INTRODUCTION

The left-right (LR) symmetric extension of the standard model (SM) [1–5] provides a natural setup for understanding the origin of parity violation as well as the smallness of neutrino masses via the see-saw mechanism [6–10], which intrinsically connects the two energy scales. Such a framework has been revived in recent years for its potential collider implications when parity restoration in the LHC energy reach is considered. Intriguing is the possibility that neutrinoless double-beta-decay ($0\nu2\beta$) may be dominated by the W_R gauge boson exchange [11–13] and therefore lead to a signal even when the improving cosmological limit on the light neutrino masses [14,15] may prevent them from being responsible for it. This has a direct counterpart in the Keung-Senjanovic process at colliders where the very same lepton number violation can appear as same-sign leptons [16], constituting a clean signal of the right-handed (RH) gauge boson W_R, with very low background. Further, the LR setup has the capability of addressing also the dark matter issue in a predictive scenario [17]. All this fertile framework triggered a number of authors to investigate both direct and indirect signatures of a TeV scale RH gauge interaction as well as constraints from flavor changing processes [18–36]. Flavor and CP violating loop processes provide a sensitive and powerful test ground for any extension of the SM. For the minimal LR model, in Ref. [21] an absolute lower bound for the LR scale of ∼2.5 TeV was obtained, in full reach of LHC direct searches. As in earlier studies, such results came essentially from the constraint on new physics contributions to ΔM_K.

In the present paper we focus again on $\Delta F = 2$ transitions of K and B mesons. Besides updating experimental data, we improve on previous analyses in two crucial respects. First, together with the LR box and the tree-level flavor-changing (FC) Higgs amplitudes, we include the leading one-loop LR renormalizations of the latter, which were neglected in recent discussions but are needed in order to obtain a gauge-independent result [37–40]. These additional contributions add constructively and play a relevant

[*]stefano.bertolini@sissa.it
[†]alessio.maiezza@ific.uv.es
[‡]fabrizio.nesti@irb.hr

role in the total amplitude. Second, we improve on the assessment of the QCD renormalization factors. In particular, the coefficient of the amplitudes with top and charm quarks exchanged in the loop was underestimated in Ref. [21].

This has a relevant implication for CP violation in K mixing where the charm-top contribution plays a crucial role in the LR model. The destructive interference between the cc and ct amplitudes, achieved by a given configuration of the relevant LR phases, is in fact more efficient than estimated in the past. As a consequence, given present data and the related uncertainties, $\Delta B = 2$ mixing and related CP violation play now a leading role in constraining low scale LR symmetry. We expect this feature to become even more prominent in the future with more data coming from LHCb and B factories, while only a substantial theoretical improvement on the calculation of the long-distance contributions to the $K_L - K_S$ mass difference may make this observable prevail over B data.

In minimal LR models a discrete symmetry is often assumed that relates the couplings in the left and right sectors, the only two realistic implementations being generalized parity ($\mathcal{P}$) and generalized charge conjugation ($\mathcal{C}$) [21,41,42]. The latter arises naturally in a grand unified SO(10) embedding as a generator of the algebra [43,44]. We analyze the impact of meson oscillations in both cases of low scale symmetry restoration.

A first outcome of our analysis is that, in the case of $\mathcal{P}$ parity, after considering the improved renormalization and the new contributions to CP violation in the K sector (ε and ε') we can strongly rule out the regime of hierarchical VEVs of the bidoublet, $v_2/v_1 < m_b/m_t \simeq 0.02$. For not so hierarchical VEVs, the predictivity of the model and the strict correlation among the LR phases requires a fully numerical analysis with constraints from K and B oscillations.

The numerical analysis leads to a reassessment of the absolute lower bounds on the LR scales. We find the FC Higgs to be bounded by B oscillations to be always above 20 TeV. Thus, as is well known [45], in order to obtain TeV scale LR symmetry the W_R gauge boson has to be substantially lighter than the second Higgs doublet, posing the concern of perturbativity of the scalar coupling to the longitudinal gauge boson components [22,23,33]. Our result is that, keeping M_H at the limit of the perturbative regime, a fit of the present B_d and B_s mixing data allows for W_R as light as 2.9(3.2) TeV at the 95% C. L. in the $\mathcal{C}(\mathcal{P})$ case.

The possibility of such a low scale of LR symmetry, favorable to LHC direct detection, is achieved in both frameworks for quite specific patterns of the model CP phases, which we discuss in detail.

We discuss finally the foreseen improvements following from the constraints on $\Delta B = 2$ observables in the upgraded stages of LHCb and Super-B factories, and conclude that they will raise the sensitivity to the LR scale beyond 6 TeV, thus setting a challenging benchmark for the direct search [the latter being sensitively dependent on the decay channels and the mass scale of the right-handed neutrinos (for a discussion see [21,46])].

II. LR MODEL AND MESON OSCILLATIONS

In the minimal LR model additional $\Delta F = 2$ transitions are mediated by the right-handed gauge boson W_R and the neutral flavor changing Higgs (FCH) H. We review the model and the relevant Lagrangian interactions in Appendix A. Here we just recall that the W_R charged-current interactions are characterized by a flavor mixing matrix V_R, that is the analogue of the standard Cabibbo-Kobayashi-Maskawa (CKM) matrix V_L.

While the W_R gauge bosons appear in loop diagrams, the FCH mediates $\Delta F = 2$ transitions at the tree level. Both W_R and H exhibit the same fermion mixing structure, proportional to $V_L^* V_R$ (see Appendix A). The phenomenological analysis of Ref. [21] shows that the mixing angles in V_R are very close to V_L, thus making the model very predictive. To the detail, the precise form V_R depends on the discrete LR symmetry realization, denoted by $\mathcal{P}$ parity and $\mathcal{C}$ conjugation,

$$\mathcal{P}\colon\ V_R \simeq K_u V_L K_d, \qquad \mathcal{C}\colon\ V_R = K_u V_L^* K_d. \tag{1}$$

$K_{u,d}$ are diagonal matrices of phases, namely $K_u = \mathrm{diag}\{e^{i\theta_u}, e^{i\theta_c}, e^{i\theta_t}\}$, $K_d = \mathrm{diag}\{e^{i\theta_d}, e^{i\theta_s}, e^{i\theta_b}\}$. For a detailed discussion see [21]. It is enough to recall that in the case of $\mathcal{C}$, the additional CP phases are independent parameters, while in the case of $\mathcal{P}$ they are related since the theory has just one free parametric phase beyond the CKM one. In the latter case an analytic solution was provided in Ref. [20] which holds however in a specific limit of the model Lagrangian parameters (see also Appendix A).

In the case of $\mathcal{C}$ the freedom of the CP phases plays a crucial role in evading the stringent constraints from flavor physics. Recent detailed discussions include Refs. [21] and [27].

A. Effective $\Delta F = 2$ LR Hamiltonian

In Fig. 1 all the relevant classes of LR Feynman diagrams for meson oscillations are shown. The relevant Lagrangian interactions are summarized in the appendix A. The four contributions are identified as box, tree-level flavor changing Higgs (FCH) amplitude and the related self-energy and vertex LR renormalization.

The diagrams drawn are representative of each class, all allowed contractions being understood. The Feynman amplitude A in Fig. 1 is not gauge independent but the sum of the A, B, and C amplitudes does [37,38,40]. Apparently the box and the C, D diagrams depend on different parameters (namely the H mass). On the other hand, the Higgs coupling to the charged would-be

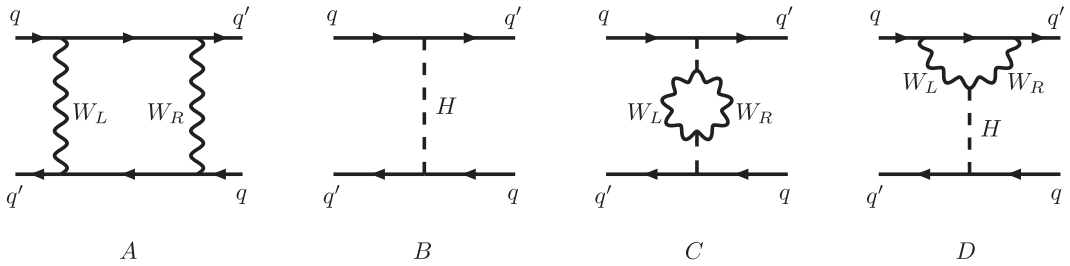

FIG. 1. The four classes of leading LR diagrams contributing to the neutral meson mixings. A, B, C, D identify the box diagrams, the H-mediated tree-level amplitude, the one-loop self-energy, and vertex renormalizations, respectively. The diagrams drawn are just representatives of each class and all allowed contractions among external and internal states are understood. In classes C and D all diagrams which do not contain the HW_LW_R vertex (with the longitudinal components of the gauge bosons) are subleading for large M_H, analogously to H exchange in the box A.

Goldstone bosons is proportional to M_H^2/M_{W_R}. This leads to a compensation of the Higgs propagator and to contributions independent on the Higgs mass. The consequences are twofold. On the one hand, the gauge dependence of the box diagram is thereby canceled; on the other hand, even for a Higgs heavier than W_R (such a setup is enforced by the presence of the tree level FCH amplitude and it is relevant to our discussion), contributions from C and D arise that are competing in size with the box amplitude. As we shall see, the presence of these contributions has a sizable effect in B-physics observables, as well as for the the kaon CP violating parameter ε.

Let us just mention that the corresponding loop diagrams with W_R replacing W_L are suppressed by $M_{W_L}^2/M_{W_R}^2$ compared to those in Fig. 1.

The calculation of the diagrams A, B, C, D gives at low energy the following effective Hamiltonians [38,40]:

$$\mathcal{H}_A = \frac{2G_F^2\beta}{\pi^2}\sum_{i,j} m_i m_j \lambda_i^{LR}\lambda_j^{RL}\eta_{ij}^A F_A(x_i,x_j,\beta)O_S \tag{2}$$

$$\mathcal{H}_B = -\frac{2\sqrt{2}G_F}{M_H^2}\sum_{i,j} m_i m_j \lambda_i^{LR}\lambda_j^{RL}\eta_{ij}^B O_S \tag{3}$$

$$\mathcal{H}_C = -\frac{G_F^2\beta}{2\pi^2 M_H^2}\sum_{i,j} m_i m_j \lambda_i^{LR}\lambda_j^{RL}\eta_{ij}^C F_C(M_{W_L},M_{W_R},M_H)O_S \tag{4}$$

$$\mathcal{H}_D = -\frac{4G_F^2\beta}{\pi^2 M_H^2}\sum_{i,j} m_i m_j \lambda_i^{LR}\lambda_j^{RL}\eta_{ij}^D F_D(m_i,m_j,M_{W_L},M_{W_R},M_H)O_S \tag{5}$$

where $\beta = M_{W_L}^2/M_{W_R}^2$, $\lambda_i^{LR} = V_{id'}^{L*}V_{id}^R$, $x_i = m_i^2/M_{W_L}^2$ and $i,j = c,t$. The dimension six operator O_S is identified with $\bar{s}Ld\bar{s}Rd$, $\bar{b}Ld\bar{b}Rd$ and $\bar{b}Ls\bar{b}Rs$ for the K, B_d and B_s meson mixings, respectively, with $R, L = (1 \pm \gamma_5)/2$. The coefficients η_{ij} encode the effect of the QCD renormalization down to the relevant hadronic scale (where the matrix elements of O_S are evaluated). Finally, the loop functions $F_{A,C,D}$ are defined in Appendix B.

A few comments are in order. A complete operator basis for the Hamiltonians in Eqs. (2)–(5) includes $O_V = \bar{d}'\gamma_\mu Ld\bar{d}'\gamma^\mu Rd$. At the leading order (LO) in the QCD resummation the anomalous dimension matrix diagonalizes on two multiplicative renormalized operators, proportional, respectively, to O_S and to $O_{\tilde{V}} = O_V + \frac{2}{3}O_S$ [40]. We verified that the QCD induced amplitude related to $O_{\tilde{V}}$ remains in all cases negligibly small compared to that of O_S (for K mixing the hadronic matrix element of O_S is chirally enhanced as well [47]). We neglect the QCD renormalization above the top mass, since it amounts to a fraction always below 10% of the whole effect. This amounts to effectively matching the amplitudes at the weak scale and it allows us to write the QCD corrected Hamiltonian in the simple form of Eqs. (2)–(5).

The two vertex (D) contractions with the loop enclosing the upper and bottom quark line, respectively, lead to an exchange of the L/R chirality in O_S. An analogous effect has the interchange of W_L and W_R in the box (A) and vertex (D) diagrams, while it does not affect the self-energy diagram. This amounts just to a multiplicity factor for the $\Delta F = 2$ transitions we are considering since the

operator O_S is symmetric for $L \leftrightarrow R$ when external momenta are neglected.

Finally, a convenient subtraction must be applied to the divergent amplitudes C and D such that M_H identifies with the one-loop pole mass [38].

The numerical relevance of the diagrams C and D compared to A depends on whether kaon or B meson mixings are considered. As a matter of fact, when the charm quark dominates the $\Delta F = 2$ amplitude (for instance when computing the CP conserving ΔM_K) since the box amplitude is enhanced by a large log (namely $\log(m_c^2/M_{W_L}^2)$) with respect to the amplitudes C and D. For such a component of the amplitude we find that the contribution to ΔM_K of $\mathcal{H}_{C+D}$ is confined to be below 20% of $\mathcal{H}_A$.

This is no longer true for CP violating observables in the kaon system, as ε, or B meson observables, where the top quark exchange leads the loop amplitudes and all diagrams compete.

B. QCD renormalization

The effective Hamiltonians are written in Eqs. (2)–(5) to hold at the scales relevant to the considered mesonic transitions, namely m_b for B and the GeV scale for kaons. The effective four-quark operators receive important QCD renormalization in their evolution from the fundamental scales. Not all needed renormalization factors are available at the next-to-leading (NLO) order for the LR Hamiltonians here discussed. On the other hand, the QCD renormalization from the left-right scales down to the weak scale (e.g., m_t) is readily estimated at LO from Ref. [40] to be a small fraction of the overall QCD correction (always below 10%). By neglecting it and matching effectively the LR amplitudes at the weak scale, the NLO η factors for the top quarks mediated diagrams (whose integration leads at the weak scale to O_S) are obtained from Ref. [48]. This is all what is needed for the discussion of $B^0 - \overline{B^0}$ mixings, where top exchange dominates the box end the vertex diagrams, A and D, respectively.

Having integrated out the heavy H scalar and the LR gauge boson states, the NLO QCD renormalization of the tree-level FCH (B) and the self-energy diagram C is straightforward and can be obtained from Ref. [48]. As a matter of fact, the running up-quark masses present in the flavor-changing Hdd' couplings (see Appendix B) absorb the QCD renormalization of O_S down to the decoupling quark scale, leaving the residual QCD renormalization of the effective operator down to the hadronic scale (the LO anomalous dimension of O_S is minus twice that of a mass).

The case of the box diagrams with one or two intermediate charm quarks can be handled according to the procedure described in [40,49], and partly by using the results of Ref. [48]. We verified that, when both calculations can be compared (e.g., for the $t-t$ amplitudes), implementing the NLO running coupling in the LO approach of [40] approximates well (within 20%) the NLO results given in [48]. In such a case we use the NLO values derived from Ref. [48].

TABLE I. QCD renormalization factors for kaon and B mixing as described in the text. They are computed at $\mu = 1$ GeV and m_b for K and B, respectively, for central values of the parameters. The observables here discussed are mainly sensitive to $\eta_{\mathrm{Kcc,ct}}$ and η_{Btt}.

	η_{Kcc}	$\eta_{\mathrm{Kct,tc}}$	η_{Ktt}	η_{Bcc}	$\eta_{\mathrm{Bct,tc}}$	η_{Btt}
A	1.15	2.23	5.63	0.52	1.01	2.25
B, C, D	1.26	2.66	5.63	0.50	1.10	2.25

The QCD renormalization of the vertex diagram (D) with internal charm can be evaluated analogously. The absence of large logs in the Wilson coefficient (see Appendix B) leads, in the LO approach of Ref. [40], to a QCD correction identical to that of the B and C diagrams.

The numerical values of the η_{QCD} coefficients thereby obtained are reported in Table I. Since the LO anomalous dimension of O_S equals up to the sign that of m_i^2, a large part of the QCD renormalization is absorbed by the running quark masses in the $m_i m_j$ pre-factor. This justifies the size pattern of the QCD renormalization factors in the table. The errors due to the uncertainties in the input parameters (strong coupling and mass thresholds) are as well reduced by the same mechanism amounting to a maximum of 10% in η_{Ktt} and of 5% in η_{Btt} [48]. These uncertainties are included in the conservative ranges we shall consider for the LR contributions to the relevant observables. It is worth noting that well within the uncertainty of the [40] LO calculation (α_s^{NLO} improved) the box $\eta_{\mathrm{cc,ct}}$ coefficients are identical to the corresponding coefficients of the H self-energy and vertex amplitudes.

C. Hadronic matrix elements

The hadronic matrix elements of the operators O_S can be readily evaluated by factorization via the vacuum saturation approximation (VSA). One obtains

$$\begin{aligned}
\langle \overline{K^0}|\bar{s}Ld\bar{s}Rd|K^0\rangle &= \frac{1}{2} f_K^2 m_K \mathcal{B}_4^K \left[\frac{m_K^2}{(m_s+m_d)^2} + \frac{1}{6}\right] \\
\langle \overline{B_d^0}|\bar{b}Ld\bar{b}Rd|B_d^0\rangle &= \frac{1}{2} f_{B_d}^2 m_{B_d} \mathcal{B}_4^{B_d} \left[\frac{m_{B_d}^2}{(m_b+m_d)^2} + \frac{1}{6}\right] \\
\langle \overline{B_s^0}|\bar{b}Ls\bar{b}Rs|B_s^0\rangle &= \frac{1}{2} f_{B_s}^2 m_{B_s} \mathcal{B}_4^{B_s} \left[\frac{m_{B_s}^2}{(m_b+m_s)^2} + \frac{1}{6}\right] \qquad (6)
\end{aligned}$$

where f_{K,B_d,B_s} and m_{K,B_d,B_s} are the decay constants and the masses of the mesons K and $B_{d,s}$, respectively. The bag factors $\mathcal{B}_4^M$ parametrize the deviation from the naive VSA. The first unquenched lattice determinations have appeared in 2012 [50,51]. A more recent lattice calculation using staggered fermions has found discrepant results [52]. In particular, a value of $\mathcal{B}_4^M$ about 50% larger. The origin of

TABLE II. Running quark masses and relevant bag parameters used in the computation. The numerical values are given at the NLO in the $\overline{\text{MS}}$(NDR) scheme. Errors in the last figures are reported in the round brackets.

Parameters	Input values
$m_t(m_t)$	164(1) GeV
$m_b(m_b)$	4.18(3) GeV
$m_c(m_c)$	1.28(3) GeV
$m_s(2\ \text{GeV})$	0.095(5) GeV
$m_s(1\ \text{GeV})$	0.127(7) GeV
$\mathcal{B}_4^K(2\ \text{GeV})$	0.78(3)
$\mathcal{B}_4^{B_d}(m_b)$	1.15(3)
$\mathcal{B}_4^{B_s}(m_b)$	1.16(2)

this discrepancy is being currently investigated [53]. In Table II we report the values we use in our analysis [54]. The term $1/6$ in Eq. (6) is numerically subleading and it is often neglected (in the $B-\bar{B}$ matrix elements as well). This is taken accordingly into account when using the lattice bag factors in our numerical analysis.

The quark masses appearing in the matrix elements are scale dependent and they are evaluated at the relevant hadronic scales. It is worth noting that by considering the scale dependent VSA matrix elements the LR bag factors turn out with very good approximation scale independent. This is related to the m^{-2} anomalous dimension of O_S.

III. CONSTRAINTS FROM K AND B_d, B_s OSCILLATIONS

A. Parametrization of LR amplitudes

For both K and $B_{d,s}$ oscillations, it is useful to discuss the allowed NP constraints in terms of ratios of the additional contributions to the correspond SM quantities or experimental data [55–59]. We introduce the parameters

$$h_m^K \equiv \frac{2\,\text{Re}\langle\overline{K^0}|\mathcal{H}_{LR}|K^0\rangle}{(\Delta M_K)_{\text{exp}}}, \tag{7}$$

$$h_\varepsilon^K \equiv \frac{\text{Im}\langle\overline{K^0}|\mathcal{H}_{LR}|K^0\rangle}{\text{Im}\langle\overline{K^0}|\mathcal{H}_{LL}|K^0\rangle}, \tag{8}$$

$$h_q^B \equiv \frac{\langle\overline{B_q^0}|\mathcal{H}_{LR}|B_q^0\rangle}{\langle\overline{B_q^0}|\mathcal{H}_{LL}|B_q^0\rangle}, \tag{9}$$

where $\mathcal{H}_{LR}=\mathcal{H}_A+\mathcal{H}_B+\mathcal{H}_C+\mathcal{H}_D$ and $q=d,\ s$. The SM hamiltonian $\mathcal{H}_{LL}$ is reported in Appendix B. The parameters h_q^B are complex, while $h_{m,\varepsilon}^K$ are real.

The up to date experimental constraints from B meson oscillations from the data fit are reported in [59] and graphically in Fig. 2 in terms of $\Delta_q \equiv 1+h_q^B$. While the B_s data agree impressively with the SM, a marginal 1.5 σ CP deviation still remains in the B_d data. In the following we shall fit the LR $\Delta F=2$ amplitudes within the given σ contours and exhibit the correlated constraints on the relevant mass scales and mixing parameters.

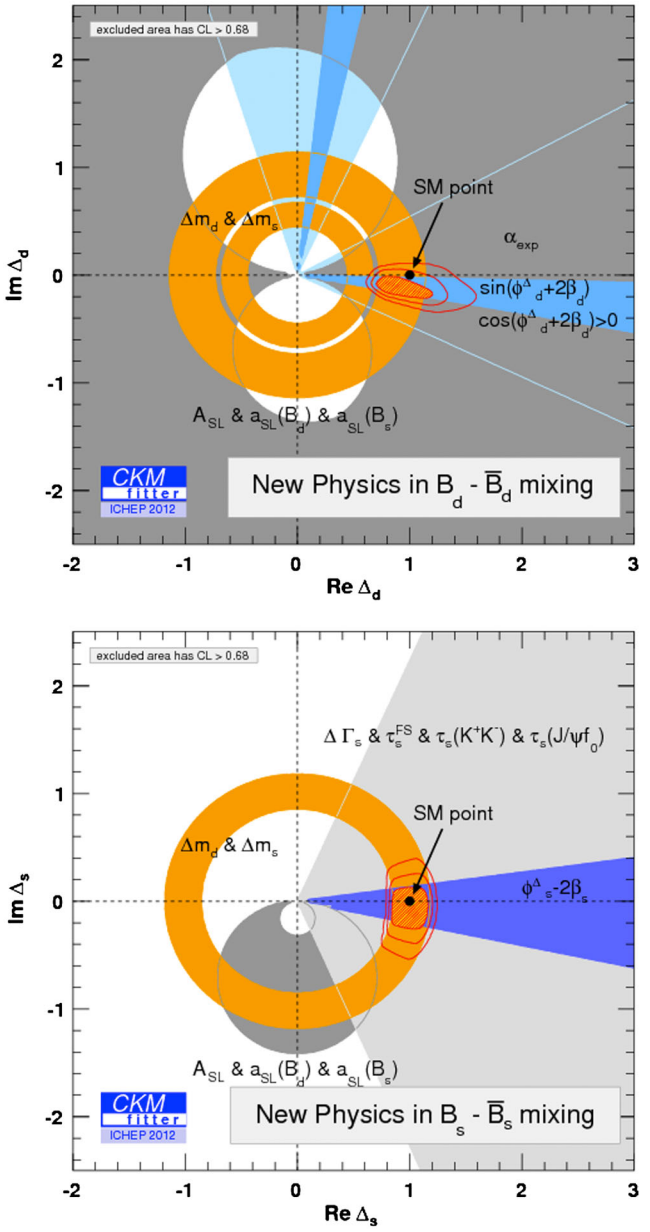

FIG. 2 (color online). Present CKM fitter constraints on $\Delta_q \equiv 1+h_q^B$ for $q=d,\ s$. From [59].

A recent discussion of the SM prediction of ε_K and the related uncertainties is found in Ref. [60]. We will conservatively allow $|h_\varepsilon^K|$ to vary within a 20% symmetric range.

More uncertain is the SM prediction of ΔM_K, with equal sharing among short-distance (SD) and long-distance (LD) theoretical uncertainties as we recap in the following section.

B. Theoretical uncertainties in ΔM_K

The up to date SD prediction of ΔM_K within the SM falls just short of the experimental value and amounts to $(0.9 \pm 0.3)\Delta M_K^{\rm exp}$ [61–64], where the error is mainly due to the large uncertainty exhibited by the SM $\eta_{\rm cc} = 1.87(76)$ parameter which is now available at the next-to-next-to-leading order (NNLO) [64] in the QCD leading log resummation. The size of this crucial parameter has increased by 36% compared to the NLO calculation, bringing the SD contribution in the ballpark of the experimental value (with some worry on the convergence of the expansion accounted for in the large error).

On the other hand, it is well known that potentially large LD contributions have to be included as well. A very recent reassessment of such a LD contributions in the large N expansion is presented in Ref. [65]. By including $1/N$ corrections the authors find $\Delta M_K^{\rm LD} = (0.2 \pm 0.1)\Delta M_K^{\rm exp}$.

In comparison, by considering the leading pion exchange and the tree-level η' contribution one obtains $\Delta M_K^{\rm LD} = (0.1 \pm 0.2)\Delta M_K^{\rm exp}$ [66], where the uncertainty is driven by the meson loop scale dependence.

A chiral quark model prediction of $\Delta M_K^{\rm LD}$ at the NLO in the chiral expansion was performed in Ref. [67,68]. A quite stable prediction $\Delta M_K^{\rm LD} \approx -0.1\ \Delta M_K^{\rm exp}$ was found, where the negative value is driven by nonfactorizable gluon condensate corrections to the $\Delta S = 1$ chiral coefficients.

Quite recently a full lattice calculation of ΔM_K on a $2+1$ flavor domain wall fermion, has appeared [69,70] that accounts for $(0.95 \pm 0.1)\Delta M_K^{\rm exp}$. Such a result, taken at face value (the quoted error is statistical), very tightly constrains new physics contributions. On the other hand it is obtained with kinematics still away from physical and further developments are called for.

In view of the distribution and the theoretical uncertainties related to the SD and LD components we may conservatively consider a 50% range of $\Delta M_K^{\rm exp}$ still available for new physics contributions, even though the recent SD and LD developments hint to a smaller fraction of the experimental value.

C. Numerical results

In this section we conveniently use the parameters h in Eqs. (7)–(9) in order to apply the experimental constraints on the new physics contributions and to obtain the corresponding bounds on the LR scales. Such bounds are set as a correlated constraint on the $M_{W_R} - M_H$ plane, once the relevant LR parameters are marginalized. We should keep in mind that the heavy Higgs H cannot be decoupled while keeping its couplings to the LR would-be Goldstone bosons perturbative. Just by naive dimensional inspection of the effective coupling one must require $M_H/M_{W_R} < 10$ (a better, process-dependent assessment based on the convergence of the perturbative expansion confirms such an expectation [38]). In the following we choose to remain safely within the nonperturbative regime and exclude the region of M_H above $8M_{W_R}$ denoted by a gray smoothed shading in the plots. We discuss separately the $\mathcal{C}$ and $\mathcal{P}$ scenarios.

1. Low scale left-right $\mathcal{C}$ conjugation

a. $\Delta s = 2$ *observables*

We shall begin our discussion with the observables related to $K^0 - \overline{K^0}$ mixing. The impact of the vertex and self-energies diagrams in Fig. 1 is for the CP conserving observable ΔM_K accidentally low, ranging from 10% to 20% of the LR box amplitude. This is well understood because of the $\log(x_c)$ enhancement in the box loop function $F_A(x_c, x_c)$ (see Appendix B), not present in the vertex and self-energy amplitudes.

On the other hand, for the ct and tt components one expects the vertex and self-energy amplitudes to be similar in size to the corresponding LR box amplitude and they play indeed a crucial role, since they add up coherently to the box and tree amplitudes. This feature holds independently of the heavy Higgs mass, since, as already discussed, there are components of the C and D amplitudes that do not depend on the Higgs mass (they are in fact needed for the cancelation of the gauge dependence of the box diagram [38]).

In Fig. 3 we present the constraints due to the LR contributions to ΔM_K, whose SM prediction and related uncertainties were summarized in Sec. III B. The figures are correlated plots in the $M_H - M_{W_R}$ plane for the two phase configurations $\theta_c - \theta_t = 0$ or π, which lead to constructive or destructive interference between the cc and ct contributions.

The destructive interference between the cc and ct amplitudes is now much more effective when compared to the results of Ref. [21]. This is a combined effect of the presence of the additional vertex and self-energy amplitudes and of the proper evaluation of $\eta_{\rm Kct,tc}$ in Table I. The latter were underestimated by a factor of 4 in [21].

As a result, the case of $\theta_c - \theta_t = \pi$ (right plot in Fig. 3) leads to the more favorable case: one infers $M_{W_R} > 2.6(3.4)$TeV when one allows for a 50% (30%) LR contribution to ΔM_K (see the discussion in Sec. III B).

The analysis of indirect CP violation in K oscillations, characterized by ε, leads to important results. In the case of $\mathcal{C}$ conjugation the dominant LR contributions to the h_ε^K can be written in the form

$$h_\varepsilon^K \simeq {\rm Im}[e^{i(\theta_d - \theta_s)}(A_{\rm cc} + A_{\rm ct}\cos(\theta_c - \theta_t + \phi))], \qquad (10)$$

where $\phi = \arg(V_{\rm Ltd}) \simeq -22^\circ$. $A_{\rm cc,ct}$ are to an extremely good approximation real numbers (we suppressed the minor tt contribution for simplicity). For M_{W_R} in the TeV range we obtain $A_{\rm ct}/A_{\rm cc} \simeq 0.45$, with $A_{\rm cc} \simeq 90$. Analogously to the ΔM_K discussion, the phase difference $\theta_c - \theta_t$ determines the constructive or destructive interference between the cc and ct amplitudes.

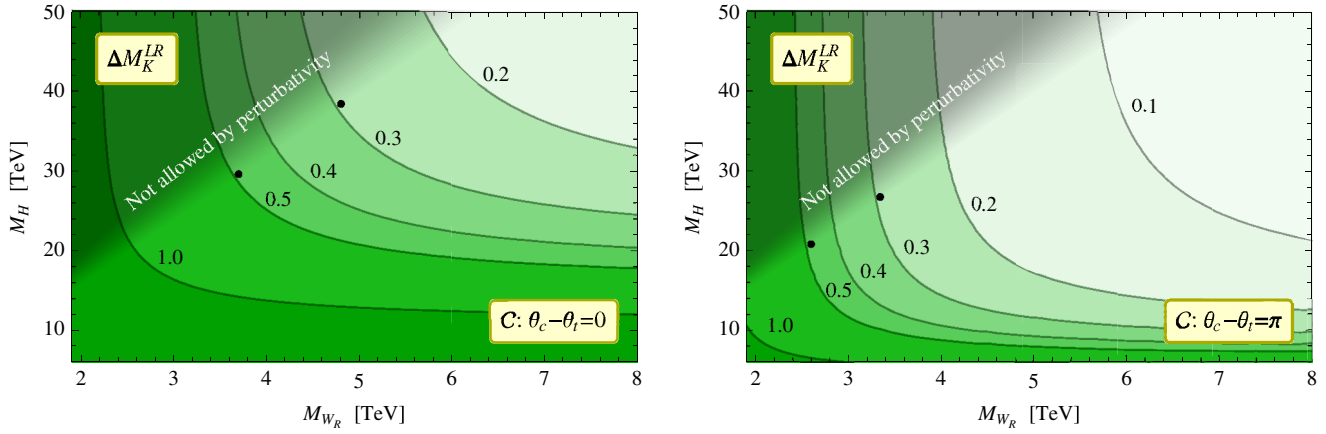

FIG. 3 (color online). Correlated lower bounds on M_{W_R} and M_H from $|\Delta M_K^{\rm LR}|/\Delta M_K^{\rm exp} < 1.0, \ldots, 0.1$ and for $\theta_c - \theta_t = 0$ (left) or π (right). The latter, respectively, denote constructive and destructive interference between the leading cc and the ct amplitudes.

The total amplitudes are sizable and the overall phase $\theta_d - \theta_s$ has to be tuned to reduce the LR contribution within the allowed limits (we require $|h_\varepsilon^K| < 0.2$ [60]). This means that ε does not lead to a bound on M_{W_R} but rather to a constraint on the phase $\theta_d - \theta_s$ [20,21]. This is shown in Fig. 4 as a correlated plot between $\theta_d - \theta_s$ and M_{W_R} for $M_H = 6\, M_{W_R}$. We show the case relative to $\theta_c - \theta_t = \pi$, the most favorable configuration for low scale LR inferred from the Δ_{M_K} discussion, but a very similar result holds for $\theta_c - \theta_t = 0$. From Eqs. (13)–(10) it is clear that plot is periodic in $|\theta_d - \theta_s|$ by π. The constraint, evident from the shaded regions in Fig. 4, is that for M_{W_R} in the TeV range $|\theta_d - \theta_s|$ has to be very small [see Eq. (10)], within a few per mil near 0 or π.

Regarding ε', in the minimal LR model one finds, by including the chromomagnetic penguin contribution [27] and updated LR matrix elements [32],

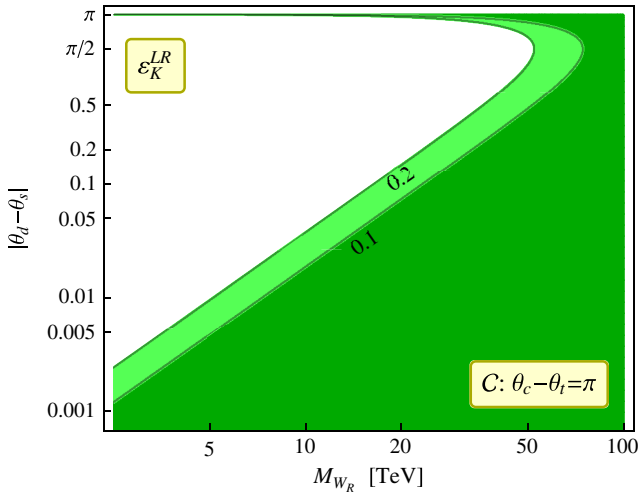

FIG. 4 (color online). Constraints on the phase $|\theta_d - \theta_s|$ versus M_{W_R}, following from the LR contributions to ε in the case of $\mathcal{C}$ as LR symmetry for $\theta_c - \theta_t = \pi$ and $h_\varepsilon^K < 0.2$ (light shading) and 0.1 (dark shading). For definiteness, we have set $M_H = 6\, M_{W_R}$. The plot is periodic for $|\theta_d - \theta_s| \to |\theta_d - \theta_s| + \pi$.

$$\begin{aligned}\varepsilon'_{\rm LR} \simeq\ & |\zeta| 2.73 [\sin(\alpha - \theta_u - \theta_d) + \sin(\alpha - \theta_u - \theta_s)] \\ & + |\zeta| 0.008 [\sin(\alpha - \theta_c - \theta_d) + \sin(\alpha - \theta_c - \theta_s)] \\ & + \beta 0.030 \sin(\theta_d - \theta_s), \end{aligned} \tag{11}$$

where ζ is the $W_L - W_R$ mixing $\simeq -\beta e^{i\alpha} \frac{2x}{1+x^2}$, with x the modulus of the ratio of the Higgs bidoublet VEVs, and α their relative phase (see Appendix A). The first line in Eq. (11) is due to the current-current $Q_{1,2}^{\rm LR,RL}$ operators, the second to the chromomagnetic LR penguins $Q_g^{L,R}$, and the last line to the current-current $Q_{1,2}^{\rm RR}$ operators (see Ref. [27] for notation and details). This expression will be used also below in the case of $\mathcal{P}$.

In the case of $\mathcal{C}$, the conclusion is straightforward: the constraint from ε' can be satisfied by either having small enough LR-mixing ζ (via x) or, alternatively, by having phases $\simeq 0$ or π, which suppress altogether CP violation. It is indeed a general fact [21] that in the case of $\mathcal{C}$ the constraints from CP violation can be satisfied by the freedom in the CP-phases, thus allowing the LR symmetry at the TeV scale.

b. $\Delta b = 2$ *observables*

The analysis of $B_{d,s}$ mixing is substantially affected by the presence of diagrams C and D of Fig. 1. In fact, the loop amplitudes are dominated by the top quark exchange, thus the LR box diagram is no longer logarithmically enhanced and the $W_L - W_R$ renormalization diagrams lead to relevant additions, typically of the same order (independently from the heavy Higgs mass, as we discussed).

It turns out that in spite of the absence of the log and chiral enhancements present in the kaon case, B mixing is sensitive to LR multi-Tev scales. In addition to a numerical factor O(10) in the Wilson coefficient functions, the LR hamiltonian exhibits, when compared to the SM, a factor of $4 \sim m_t^2/m_{W_L}^2$ due to the needed helicity flips on the top quark propagator, and a further factor of 4 from the ratio of the QCD factors (compare Eqs. (2)–(5) and the results in Appendix B). Finally, the coherent presence of the

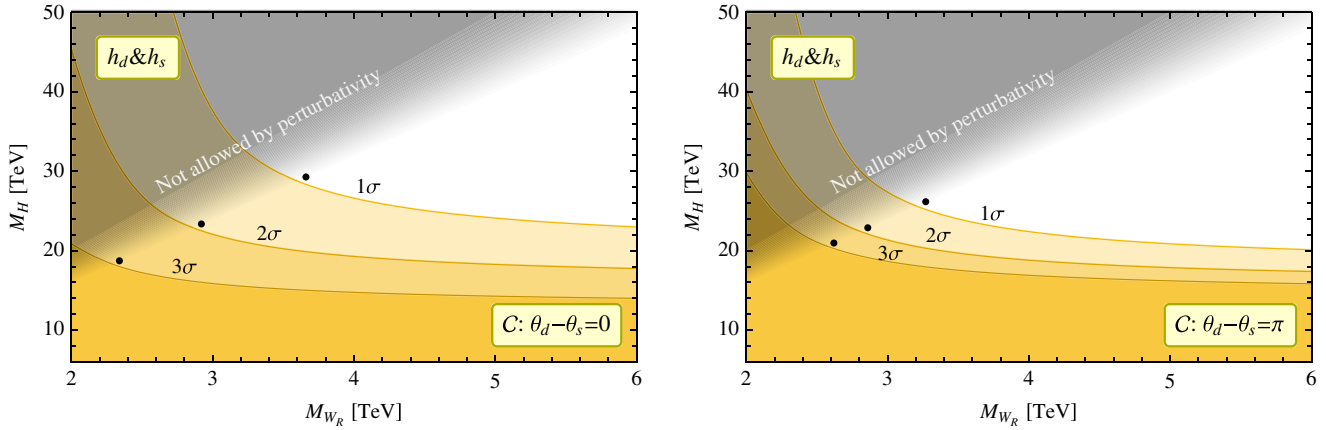

FIG. 5 (color online). Combined constraints in the $\mathcal{C}$ case on M_H and M_{W_R} from the B_d and B_s mixings according to the experimental bounds in Fig. 2, for $\theta_d - \theta_s = 0$ (left) and $\theta_d - \theta_s = \pi$ (right), as required by ε.

tree-level FC Higgs contribution and its one-loop renormalization add, even for a heavy H, another factor $3-4$. All in all these numerical enhancements make the $\Delta b = 2$ observables sensitive to a W_R mass in the multi TeV range. This is a case where a naive analysis based on the relevant effective operators would be likely misleading.

We analyze the constraints from B_d and B_s mixings by means of the parameters $h_{d,s}$ in Eq. (9). They are complex and, while their moduli are controlled by M_H and M_{W_R}, in the $\mathcal{C}$-conjugation scenario their phases are related. By taking into account that $\theta_d - \theta_s \simeq 0,\ \pi$ from the previous discussion, we can parametrize both $h_{d,s}$ by the same free combination of phases $\theta_d - \theta_b$, namely,

$$h_d \sim -e^{i(\theta_d-\theta_b-2\phi)}, \qquad h_s \sim \mp e^{i(\theta_d-\theta_b)}, \tag{12}$$

where again $2\phi = 2\arg(V_L)_{td} \simeq -44^\circ$ and the sign $\mp$ follows from $\theta_d - \theta_s \simeq 0$ or π, respectively. The numerical analysis requires to marginalize over $\theta_d - \theta_b$, by fitting in both B_d and B_s constraints in Fig. 2.

Our results are shown in Fig. 5, the left and the right plots corresponding to $\theta_d - \theta_s = 0,\ \pi$, respectively. The latter configuration minimizes the LR scale and we obtain $M_{W_R} > 2.9 - 3.3$ TeV, at 2 and $1\,\sigma$ C.L., respectively. It is worth mentioning that presently the experimental data on B_d mixing [59] show a mild $1.5\,\sigma$ discrepancy with the SM

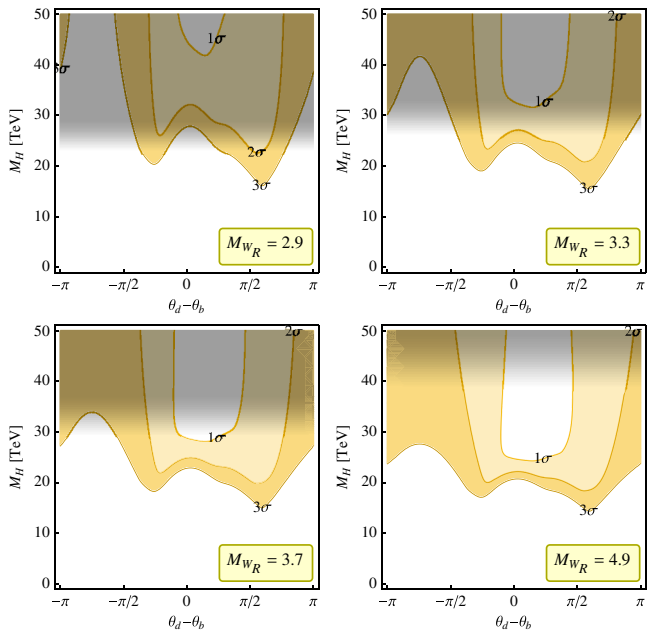

FIG. 6 (color online). Allowed region of M_H and $\theta_d - \theta_b$ (above the contours and below the shading) for $\theta_d - \theta_s = 0$ and various values of M_{W_R}, as obtained from the B_d, B_s oscillation data at different confidence levels.

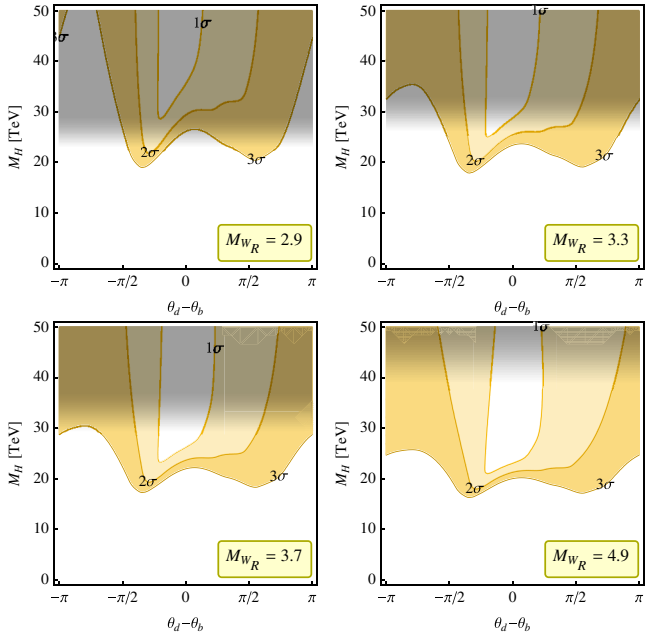

FIG. 7 (color online). Allowed region of M_H and $\theta_d - \theta_b$ (above the contours and below the shading) for $\theta_d - \theta_s = \pi$ and various values of M_{W_R}, as obtained from the B_d, B_s oscillation data at different confidence levels.

TABLE III. Summary of correlated bounds on the LR scale (in TeV) in the $\mathcal{C}$ case, for two benchmark requirements of h^K, h^B and of the relative patterns of LR phases. The limits where the B-mixing constraints prevail over K mixing are marked in bold. These represent the most conservative bounds ($M_H \gg M_{W_R}$). The absolute lower bound is $M_{W_R} > 2.9$TeV and there a preferred value of $\theta_d - \theta_b \simeq -1.7$ or 0.9 emerges, depending on $\theta_d - \theta_s$.

$\lvert h^B_{d,s}\rvert$	$\lvert h^K_m\rvert$	$\theta_c - \theta_t$	$\theta_d - \theta_s$	$\theta_d - \theta_b$	$M^{\min}_{W_R}$[TeV]
$< 2\sigma$	< 0.5	0	$\simeq 0$	$-0.8 \div 2.4$	3.7
			$\simeq \pi$	$-1.3 \div 1.8$	3.7
		π	$\simeq 0$	$\simeq 1.7$	**2.9**
			$\simeq \pi$	$\simeq -0.9$	**2.9**
$< 1\sigma$	< 0.3	0	$\simeq 0$	$-0.2 \div 1.5$	4.9
			$\simeq \pi$	$-0.5 \div 0.8$	4.9
		π	$\simeq 0$	$\simeq 0.5$	**3.7**
			$\simeq \pi$	$\simeq -0.7$	**3.3**

prediction and the LR model helps to lighten the tension to below 1σ.

It is remarkable that the bounds on the LR scale from B physics turn out to be competitive or even stronger than those obtained from kaon physics. This is due partly to the improvements of the data and partly to the due inclusion of all relevant contributions, while large LD uncertainties still affect the SM prediction of ΔM_K. It is worth mentioning that, since h_d deviates at present by $1.5\,\sigma$ from 0 (the SM value), the requirement that LR contributions make the theory consistent with the 1σ experimental region would call for $M_{W_R} < 8.0$ TeV, still in the limit of large M_H.

For either choice $\theta_d - \theta_s = 0, \pi$ we also scan the allowed ranges of the free model phase $\theta_d - \theta_b$. These are shown in Figs. 6–7, respectively, in the $M_H - (\theta_d - \theta_b)$ plane, for typical values of M_{W_R}. Depending on whether the LR scale sits onto a minimum or higher, the phase difference is sharply determined or spans a range. For $M_{W_R} \sim 5$ TeV, $\theta_d - \theta_b$ is restricted to vary from 1.5 to 2.5 at the 95% C.L.

Overall, the results are summarized in Table III for two benchmark settings of h^K, h^B and LR phases. An absolute lower bound of 2.9 TeV on M_{W_R} emerges at 95% C.L. This confirms the possibility of direct detection of the LR gauge bosons at forthcoming 14 TeV LHC run, whose sensitivity to W_R is expected to reach the 6 TeV mass threshold [71,72]. Let us remark that the bounds quoted in the Table are obtained for $M_H \gg M_{W_R}$ (still remaining in the perturbative regime for the Higgs couplings).

2. Low scale $\mathcal{P}$-parity

$\mathcal{P}$ parity in the LR symmetric model requires the Yukawa couplings Y and $\tilde{Y}$ to be Hermitian (see Appendix A for notation). The right-handed mixing matrix is given by $V_R \simeq K_u V_L K_d$ with $K_{u,d}$ diagonal matrices of phases. On the other hand, any additional CP violation (i.e., beyond CKM) arises from a nonzero relative phase (α) between the two doublet VEVs, that is the only source of non-Hermiticity of the quark mass matrices. In the limit of small ratio of the doublet VEVs ($x \equiv v_2/v_1 \ll 1$) an analytical solution can be found [20], and all phases are parametrized in terms of $x \sin\alpha$. In particular for $x \ll m_b/m_t$, all LR phases are bounded in a small range about 0 or π.

One would be tempted to conclude, as for the $\mathcal{C}$ case, that in this regime $\mathcal{P}$ parity is a viable setup for low scale LR symmetry. However, due to the different relation between the left-handed and right handed mixing matrices, the dependence of observables on the CP phases differs in the $\mathcal{P}$ and $\mathcal{C}$ schemes. In particular, for $\Delta S = 2$ mixing one obtains

$$\langle \overline{K^0}|\mathcal{H}_{\rm LR}|K^0\rangle \propto e^{i(\theta_d-\theta_s)}[A_{\rm cc} + A_{\rm ct}e^{i\phi}\cos(\theta_c - \theta_t)], \quad (13)$$

while in the case of B mixing the parameters $h_{d,s}$ read

$$h_d \sim -e^{i(\theta_d-\theta_b)}, \qquad h_s \sim -e^{i(\theta_s-\theta_b)}, \quad (14)$$

because the CKM phase $\arg(V_{\rm Ltd})$ cancels in the ratio of the LR and SM leading (tt) amplitudes. For $\theta_d - \theta_s \simeq 0, \pi$ the complex vectors h_d and h_s are approximately aligned. On the other hand, as far as the direct CP violation parameter ε' is concerned, Eq. (11) holds in both $\mathcal{C}$ and $\mathcal{P}$ cases since the top mediated LR amplitudes turn out to be subleading [27].

Let us first discuss the constraint from ε. The interplay in Eq. (13) of the overall LR phase $\theta_d - \theta_s$ and the CKM phase in the ct part of the amplitude leads to the pattern shown in Fig. 8, to be compared with Fig. 4 in the $\mathcal{C}$ case. As it appears, for $M_{W_R} < 10$ TeV one is led to the narrow result of $|\theta_d - \theta_s| \simeq 0.17$ (modulo π). (An analogous pattern is obtained for $|\theta_c - \theta_t| \simeq 0$.)

This is a fairly large phase, the reason for which being the large ratio $A_{\rm ct}/A_{\rm cc} \simeq 0.45$ in Eq. (13) combined with

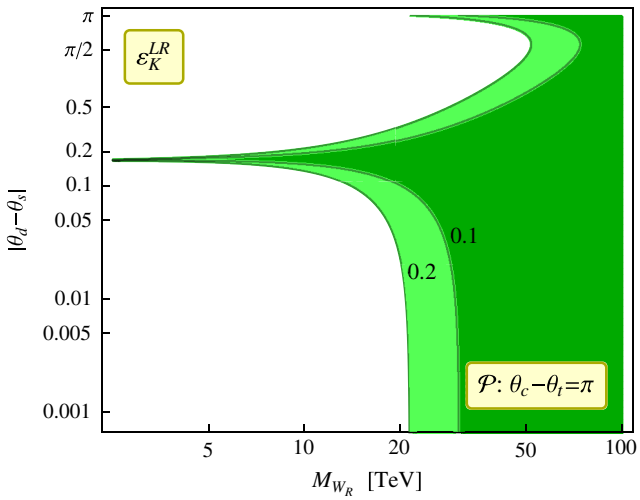

FIG. 8 (color online). Constraints on the phase $|\theta_d - \theta_s|$ versus M_{W_R}, following from the LR contributions to ε in the case of $\mathcal{P}$-parity for $\theta_c - \theta_t = \pi$, and for $h^K_\varepsilon < 0.2$ (light shading) and 0.1 (dark shading). For definiteness, we have set $M_H = 6\, M_{W_R}$. The plot is periodic for $|\theta_d - \theta_s| \to |\theta_d - \theta_s| + \pi$.

the CKM phase $e^{i\phi}$. The resulting large imaginary part in h_ε^K can only be canceled by a fairly large $\theta_d - \theta_s$ phase.

This is a crucial change with respect to the analysis in [20,21] where A_{ct}/A_{cc} resulted much smaller so that the phase $|\theta_d - \theta_s|$ was constrained to be $\simeq 0, \pi$ at the percent level. As already mentioned such a crucially different result has two distinct and comparable origins: a QCD factor η_{ct}^{LR} larger by a factor 4, underestimated in previous analyses, and the neglected contributions of the self-energy and vertex renormalization diagrams, which additionally increase the ratio A_{ct}/A_{cc} by approximately a factor 3.

The consequences of this large phase are important: first, in the regime $x \ll m_b/m_t$ where analytical expressions for the phases are available [20], it is straightforward to see using Eq. (11) that a strong bound emerges from ε', which excludes the scenario of low scale $\mathcal{P}$ LR symmetry. One finds

$$x \ll \frac{m_b}{m_t} \Rightarrow \frac{\varepsilon'_{LR}}{\varepsilon'_{exp}} \simeq \left(\frac{10\ \text{TeV}}{M_{W_R}}\right)^2, \tag{15}$$

which translates into 14(10) TeV if one tolerates a 50(100)% contribution to ε'. As a result, one can exclude the regime of hierarchic VEVs $x = v_2/v_1 \ll m_b/m_t$ for low scale $\mathcal{P}$ LR symmetry. This has also implications for the analysis of the leptonic sector [73].

On the other hand, when the ratio of the doublet VEVs is larger than a percent, the analytic solution in [20] does not apply, and one expects that for given values of x and α of order one, the spectrum of the LR phases may exhibit also large values. In order to address this problem we performed a full numerical analysis of the K and B observables here discussed. The procedure consists in a χ^2 fit of the known spectrum of charged fermions masses and mixings, together with the constraints from ε, ε' and h_d, h_s for the B mesons. The results can be summarized as follows:

(1) We confirm that for small $x < 0.02(0.01) \simeq m_b/m_t$ the model can not accommodate at the same time ε and ε' (the tension being at $2(3)\sigma$). This confirms our discussion based on the analytic approximation of Ref. [20].

(2) The tension is resolved only for larger $x > 0.02$. In this case, x becomes also irrelevant and good fits can be found regardless of x. The solution requires a definite pattern of phases: $\theta_c - \theta_t \simeq \pi/2$ [which reduces the imaginary part in Eq. (13)] together with $\theta_d - \theta_s \simeq \pi$ [which is then necessary for ε', leading to a cancelation between the two terms in the first line of Eq. (11)].

(3) This pattern of phases leads then to a well defined bound from ΔM_K [see Eq. (13)]. This is illustrated in Fig. 9.

(4) B_d mixing data then drive $\theta_d - \theta_b \simeq \pi/4$, see Fig. 2, where the data constraint on New Physics (h_d) is weaker.

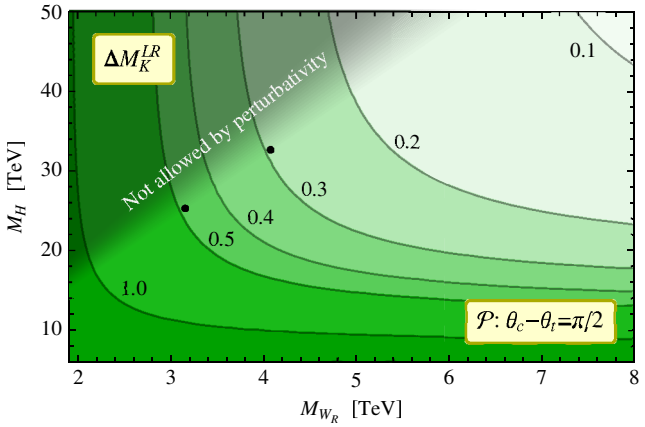

FIG. 9 (color online). Correlated bounds on M_R and M_{W_R} (region above the curves) for $|\Delta M_K^{LR}|/\Delta M_K^{exp} < 1.0, \ldots, 0.1$ and for $\theta_c - \theta_t = \pi/2$ in the case of $\mathcal{P}$ parity.

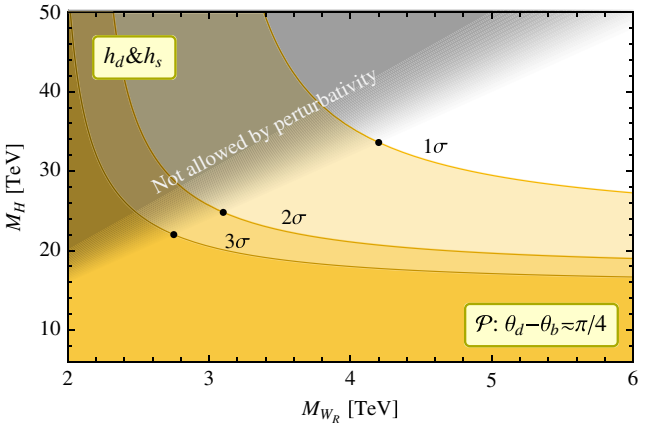

FIG. 10 (color online). Combined constraints on M_R and M_{W_R} from ε, ε' B_d and B_s mixings obtained in the $\mathcal{P}$ parity case from the numerical fit of the Yukawa sector of the model.

(5) According to this pattern we find $M_{W_R} > 3.1$ TeV at 2σ C.L. and $M_{W_R} > 4.2$ TeV at 1σ C.L., as illustrated in Fig. 10.

In summary, hierarchic VEVs $x < 0.02$ are ruled out for low scale $\mathcal{P}$ LR-symmetry, while for larger x one can find the allowed region in the $M_H - M_{W_R}$ plane, according to Figs. 9–10. Table IV summarizes the results for the LR

TABLE IV. Summary of correlated bounds on the LR scale (in TeV) in the $\mathcal{P}$-parity case, for two benchmark requirements on the h^K's and h^B's and the favorite pattern of the LR phases. With the given uncertainties the limits arising from the combined numerical fit of ε, ε', and $B_{d,s}$ mixings are today competitive with those obtained from ΔM_K (round brackets).

$\lvert h^B_{d,s}\rvert$	$\lvert h^K_m\rvert$	$\lvert\theta_c - \theta_t\rvert$	$\lvert\theta_d - \theta_s\rvert$	$\theta_d - \theta_b$	$M_{W_R}^{\min}$[TeV]
$< 2\sigma$	< 0.5	$\simeq \pi/2$	$\simeq \pi$	$\simeq \pi/4$	3.1 (**3.2**)
$< 1\sigma$	< 0.3				**4.2** (4.1)

scale in the $\mathcal{P}$ case, which we find around 3(4)TeV for the $2(1)\sigma$ benchmark settings.

IV. WHAT NEXT?

In this work we considered the combined constraints on the TeV scale minimal LR model, from $\Delta F = 2$ observables in B and K physics. We showed that the meson mixing receives significant contributions from diagrams that were neglected in past phenomenological analysis, albeit needed for a gauge invariant result. The complete calculation together with a more careful assessment of the relevant QCD renormalization factors leads to two main results: i) the exclusion of the scenario of hierarchic bidoublet VEVs, $x < 0.02$ in the case of $\mathcal{P}$-parity. ii) the competitive or prevailing role of B-mixing data in setting the lower bounds on the LR scale. Only a substantial progress in the calculation of the $K_L - K_S$ mass difference, e.g., from lattice studies) may bring the $\Delta S = 2$ observable in the forefront.

The results are summarized in Tables III and IV for two benchmark settings of h^K, h^B and LR phases. An absolute lower bound of 2.9 TeV on M_{W_R} emerges at the 95% C.L. in the case of $\mathcal{C}$. This confirms the possibility of direct detection of the LR gauge bosons at the forthcoming 14 TeV LHC run, whose sensitivity to W_R is expected to approach the 6 TeV mass threshold [71,72]. Let us remark that the bounds quoted in the tables are obtained for $M_H \gg M_{W_R}$ (still remaining in the perturbative regime for the Higgs couplings). In the case of comparable Higgs and gauge boson masses we find a lower limit always above 20 TeV.

At present, direct searches at LHC provide bounds on the right-handed W bosons that vary according to the assumptions on the right-handed neutrinos from 2.0 to 2.9 TeV [74–76]. It is remarkable that even the most conservative indirect lower bound from B meson physics is still competitive with the direct search.

Sharp improvements in the data are expected from the second LHCb run [77]. The foreseen data accumulation of LHCb and Belle II in the coming years shall improve on the present sensitivity by a factor of 2 within the decade and up to a factor of 5 by the mid 2020s. The impact of such an experimental improvement on the sensitivity to the LR scale is depicted in Fig. 11, assuming that the future data on B_d and B_s mixings will be centered on the SM values. The shown σ contours refer to the foreseen C.L. on the combination of constraints from h_d and h_s. It is noteworthy that the future sensitivity to the LR scale will reach $7 - 8$ TeV, thus exceeding the reach of the direct collider search.

The B physics offers a number of other notable probes of possible new physics, namely rare flavor changing decays as $B \to \mu^+\mu^-$, $b \to s\gamma$, $b \to s\ell^+\ell^-$, to name a few, and related CP asymmetries. A comprehensive and updated analysis of the limits on the minimal $\mathcal{P}$ and $\mathcal{C}$ LR models is currently missing, but a preliminary estimate indicates these processes to be much less constraining, due to higher backgrounds, less enhancements, or due to the involvement of the leptonic sector, which still has more freedom in the scales and CP phases. In the arena of indirect signatures a promising avenue will be the confrontation with electric dipole moments (EDM). Dedicated efforts are ongoing [78,79] for a reassessment of the limits from nucleon, atomic and leptonic EDMs.

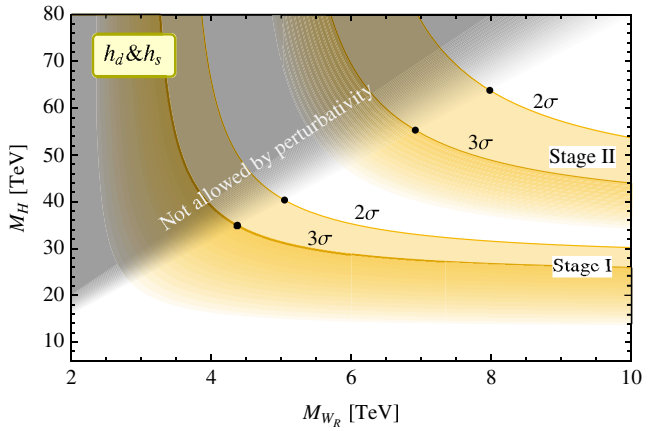

FIG. 11 (color online). Future constraints on M_R and M_{W_R} from the projected combined limits on h_d and h_s discussed in Ref. [77]. Stage I corresponds to a foreseen 7 fb^{-1} (5 ab^{-1}) data accumulation by LHCb (Belle II) by the end of the decade. Stage II assumes 50 fb^{-1} (50 ab^{-1}) data by the two experiments, achievable by mid 2020's.

On the other hand, in the collider arena, in view of the forthcoming high-energy LHC run, an exhaustive appraisal and exploiting of the various signatures is still timely and compelling in order to probe the low energy parameter space of W_R and RH neutrinos.

ACKNOWLEDGMENTS

We thank Miha Nemevšek, Goran Senjanovic, and Vladimir Tello, for useful and stimulating discussions. S. B. acknowledges partial support by the Italian MIUR Grant No. 2010YJ2NYW001 and by the EU Marie Curie ITN UNILHC Grant No. PITN-GA-2009-237920. The work of A. M. was supported in part by the Spanish Government and ERDF funds from the EU Commission [Grants No. FPA2011-23778, No. CSD2007-00042 (Consolider Project CPAN)] and by Generalitat Valenciana under Grant No. PROMETEOII/2013/007.

APPENDIX A: THE LEFT-RIGHT MODEL

1. The gauge Lagrangian

The minimal LR symmetric extension of the standard electroweak theory is based on the gauge group [1–4]

$$G_{\rm LR} = SU(2)_L \times SU(2)_R \times U(1)_{B-L},$$

Left and Right quarks and leptons sit in the fundamental representations of $SU(2)_{L,R}$, $Q_{L,R}=(ud)^t_{L,R}$, $\ell_{L,R}=(\nu e)^t_{L,R}$, with electric charges $Q=I_{3L}+I_{3R}+\frac{B-L}{2}$, where $I_{3L,R}$ are the third generators of $SU(2)_{L,R}$.

The gauge and fermion Lagrangian reads

$$\mathcal{L}=i[\bar{\Psi}_L D\Psi_L+\bar{\Psi}_R D\Psi_R] -\frac{1}{4}F_{\mu\nu}F^{\mu\nu}-\frac{1}{4}G^i_{L\mu\nu}G^{i\mu\nu}_L-\frac{1}{4}G^i_{R\mu\nu}G^{i\mu\nu}_R \quad \text{(A1)}$$

where $\Psi=(Q\ell)$, $D=\gamma_\mu D^\mu$; $D_\mu=\partial_\mu-igW^i_{\mu L}\frac{\sigma^i_L}{2}-igW^i_{\mu R}\frac{\sigma^i_R}{2}-ig'B_\mu$ is the $G_{\rm LR}$ covariant derivative ($g_L=g_R=g$). $F_{\mu\nu}=\partial_\mu B_\nu-\partial_\nu B_\mu$ and $G^i_{\mu\nu L,R}=\partial_\mu W^i_{\nu L,R}-\partial_\nu W^i_{\mu L,R}+g\epsilon^{ijk}W^j_{\mu L,R}W^k_{\nu L,R}$ are the LR gauge field tensors.

2. The Higgs sector

The scalar sector contains minimally one right and one left triplet $\Delta_R\in(1_L,3_R,2)$ and $\Delta_L\in(3_L,1_R,2)$ together with one bidoublet field $\Phi\in(2_L,2_R,0)$ [4,5]:

$$\Delta=\begin{bmatrix}\Delta^+/\sqrt{2} & \Delta^{++}\\ \Delta^0 & -\Delta^+/\sqrt{2}\end{bmatrix},\qquad \Phi=\begin{bmatrix}\phi^0_1 & \phi^+_2\\ \phi^-_1 & \phi^0_2\end{bmatrix} \quad \text{(A2)}$$

The spontaneous symmetry breaking (SSB) of $G_{\rm LR}$ to $SU(3)_C\times U(1)_Q$ is achieved by

$$\langle\Delta^0_L\rangle=v_L,\qquad \langle\Delta^0_R\rangle=v_R,\qquad \langle\Phi\rangle=\begin{bmatrix}v_1 & 0\\ 0 & v_2e^{i\alpha}\end{bmatrix}, \quad \text{(A3)}$$

where $v_L\propto v^2/v_R$ ($v=\sqrt{v_1^2+v_2^2}$). In the broken vacuum we have

$$M^2_{W_L}\simeq g^2\tfrac{v^2}{4},\quad M^2_{Z_L}\simeq\tfrac{g^2}{c_W^2}\tfrac{v^2}{4}$$
$$M^2_{W_R}\simeq g^2v_R^2,\quad M^2_{Z_R}\simeq\tfrac{g^2}{c_W^2}\tfrac{c_W^4|v_R|^2}{c_W^2-s_W^2}, \quad \text{(A4)}$$

where c_W, s_W stand for $\cos\theta_W$, $\sin\theta_W$, with θ_W the Weinberg angle.

The Yukawa Lagrangian reads

$$\mathcal{L}_Y=\bar{Q}_L(Y\Phi+\tilde{Y}\tilde{\Phi})Q_R+\text{H.c.}, \quad \text{(A5)}$$

and through the vacuum in Eq. (A3) leads to the following quark mass matrices:

$$M_u=v(Yc+\tilde{Y}se^{-i\alpha})$$
$$M_d=v(Yse^{i\alpha}+\tilde{Y}c), \quad \text{(A6)}$$

where $s=v_2/v$, $c=v_1/v$.

The diagonal mass matrices $\hat{M}_q$ are obtained as

$$M_u=U_{uL}\hat{M}_uU^\dagger_{uR},\qquad M_d=U_{dL}\hat{M}_dU^\dagger_{dR}. \quad \text{(A7)}$$

and the induced flavor mixings in the L, R charged currents are parametrized as

$$\mathcal{L}_{\rm CC}=\frac{g}{\sqrt{2}}[W^\mu_L\bar{u}_{Li}(V_L)_{ij}\gamma_\mu d_{Lj}+(L\to R)]+\text{H.c.}, \quad \text{(A8)}$$

where $V_{L,R}=U^\dagger_{uL,R}U_{dL,R}$ and i, j are flavor indices.

Relevant to our discussion is the presence in the scalar sector of the "heavy" Higgs doublet H. In terms of the fields $\phi_{1,2}$ it is given by $H=c\phi_2-se^{i\alpha}\phi_1$. From Eq. (A5) one readily shows that the tree level H^0-fermion interaction can then be written as

$$\mathcal{L}_H\simeq\frac{g}{2M_{W_L}}[\bar{u}_L(V_L\hat{M}_dV^\dagger_R)u_RH^0 +\bar{d}_L(V^\dagger_L\hat{M}_uV_R)d_RH^{0*}]+\text{H.c.} \quad \text{(A9)}$$

Notice that the $H^0\bar{q}q$ couplings are proportional to the masses of the opposite isospin quarks.

3. Discrete LR symmetries

The pattern of the left and right mixing matrices is constrained by imposing upon the model a discrete LR symmetry, which is spontaneously broken together with $SU(2)_R$. Two realistic implementations are given by the so called generalized parity $\mathcal{P}$ and conjugation $\mathcal{C}$ (see Ref. [21] for a detailed discussion) defined as

$$\mathcal{P}:\begin{cases}Q_L\leftrightarrow Q_R\\ \Phi\to\Phi^\dagger\end{cases},\qquad \mathcal{C}:\begin{cases}Q_L\leftrightarrow(Q_R)^c\\ \Phi\to\Phi^T\end{cases} \quad \text{(A10)}$$

The LR charge conjugation $\mathcal{C}$ arises naturally in a grand unified embedding as part of the $SO(10)$ algebra. Imposing $\mathcal{P}$ or $\mathcal{C}$ leads to specific symmetries of the Yukawa couplings and the LR mixings. In particular one obtains $Y=Y^\dagger$ and $Y=Y^T$, respectively. In the same two settings the mixing matrices are related as in Eq. (1), respectively, by $V_R\simeq K_uV_LK_d$ and $V_R=K_uV_L^*K_d$, with $K_{u,d}$ diagonal matrices of phases. As recalled in the text, in the case of $\mathcal{C}$, these phases are free.

In the cases of $\mathcal{P}$ they are all related to a combination of the VEVs ratio v_2/v_1 and to their relative phase α. In the limit $v_2/v_1\ll m_b/m_t$ they are numerically of the order of $m_t/m_b(v_2/v_1)\sin\alpha$ [20].

APPENDIX B: LOOP FUNCTIONS

For a self-contained discussion we report here the standard $\Delta F=2$ effective Hamiltonian [80],

$$\mathcal{H}_{LL}^{\Delta F=2} = \frac{G_F^2 M_{W_L}^2}{4\pi^2} \sum_{i,j=c,t} \lambda_i^{LL} \lambda_j^{LL} \eta_{ij}^{LL} F_{LL}(x_i, x_j) O_{LL}, \quad \text{(B1)}$$

where $\lambda_i^{LL} = V_{id'}^{L*} V_{id}^{L}$, $x_i = m_i^2/M_{W_L}^2$ and $O_{LL} = \bar{d}\gamma_\mu P_L d \bar{d}\gamma^\mu P_L d$, with $\langle M^0 | O_{LL} | M^0 \rangle = \frac{2}{3} f_M^2 m_M$ in the VSA.

The calculation of the QCD renormalization factors η_{ij}^{LL} was completed at the NLO in Ref. [62] and at the NNLO in Refs. [63,64]. A summary of updated values is found in Ref. [60]. The loop function can be written as

$$F_{LL}(x_i, x_j) = f(x_i, x_j) - f(x_i, 0) - f(0, x_j) + f(0, 0) \quad \text{(B2)}$$

with

$$f(x_i, x_j) = \left(1 + \frac{x_i x_j}{4}\right) I_2(x_i, x_j, 1) - 2 x_i x_j I_1(x_i, x_j, 1) \quad \text{(B3)}$$

and

$$I_1(x_i, x_j, \beta) = \frac{x_i \ln x_i}{(1 - x_i)(1 - x_i\beta)(x_i - x_j)} + (i \leftrightarrow j) - \frac{\beta \ln \beta}{(1 - \beta)(1 - x_i\beta)(1 - x_j\beta)}, \quad \text{(B4)}$$

$$I_2(x_i, x_j, \beta) = \frac{x_i^2 \ln x_i}{(1 - x_i)(1 - x_i\beta)(x_i - x_j)} + (i \leftrightarrow j) - \frac{\ln \beta}{(1 - \beta)(1 - x_i\beta)(1 - x_j\beta)}. \quad \text{(B5)}$$

Finally we list the loop functions appearing in the leading LR Hamiltonians of Eqs. (2)–(5). The loop amplitudes correspond to the results reported in Ref. [38], with typos amended (and summed over $W_L \leftrightarrow W_R$ exchange). We identify the masses of the scalar and pseudoscalar components of the complex field H, since mass splittings, induced by the electroweak breaking, are negligible compared to the average mass scale. A convenient subtraction is applied in $\mathcal{H}_{C,D}$ that identifies M_H with the one-loop pole mass [38].

Starting with the LR analogue of the box function in Eq. (B2), we have in the 't Hooft-Veltman gauge,

$$F_A(x_i, x_j, \beta) = \left(1 + \frac{x_i x_j \beta}{4}\right) I_1(x_i, x_j, \beta) - \frac{1 + \beta}{4} I_2(x_i, x_j, \beta), \quad \text{(B6)}$$

with $\beta = M_{W_L}^2/M_{W_R}^2$, while the self-energy and vertex loop functions in $\mathcal{H}_{C,D}$ are given by [38]

$$F_C(M_{W_{L,R}}, M_H) = [10 M_{W_L}^2 M_{W_R}^2 + M_{W_L}^4 + M_{W_R}^4 + M_H^4][I_a(0) - I_a(M_H^2)]/M_H^2 + [10 M_{W_L}^2 M_{W_R}^2 + M_{W_R}^4 + M_H^4 - 2M_H^2(M_{W_L}^2 + M_{W_R}^2)] I_b(M_H^2), \quad \text{(B7)}$$

$$F_D(m_i, m_j, M_{W_{L,R}}, M_H) = 2(M_{W_L}^2 + M_{W_R}^2)[I_a(0) - I_a(M_H^2)] - \left[\frac{M_{W_L} M_{W_R} M_H^2}{1 - 4 M_{W_L} M_{W_R}/m_i^2} [K_a(0, m_i^2) - K_a(M_H^2, m_i^2)] + (i \to j)\right], \quad \text{(B8)}$$

with

$$I_a(q^2) = -\frac{i}{\pi^2} \int dk^4 \frac{1}{(k^2 - M_{W_L}^2)[(k+q)^2 - M_{W_R}^2]} \quad \text{(B9)}$$

$$I_b(q^2) = -\frac{i}{\pi^2} \int dk^4 \frac{q(k+q)}{q^2 (k^2 - M_{W_L}^2)[(k+q)^2 - M_{W_R}^2]^2} \quad \text{(B10)}$$

$$K_a(q^2, m_i^2) = -\frac{i}{\pi^2} \int dk^4 \frac{1}{[(k + \frac{q}{2})^2 - m_i^2](k^2 - M_{W_L}^2)[(k+q)^2 - M_{W_R}^2]}. \quad \text{(B11)}$$

For convenience we report the results of the integrals in Eq. (B9) in the relevant limit $m_i^2, M_{W_L}^2 \ll M_{W_R}^2 \ll M_H^2$:

$$I_a(0) - I_a(M_H^2) \approx \log \frac{M_H^2}{M_{W_R}^2} - 1 \quad \text{(B12)}$$

$$I_b(M_H^2) \approx \frac{1}{M_H^2} \quad \text{(B13)}$$

$$K(0) - K(M_H^2) \approx \frac{m_i^2 \log \frac{m_i^2}{M_{W_R}^2} - M_{W_L}^2 \log \frac{M_{W_L}^2}{M_{W_R}^2}}{M_{W_R}^2 (m_i^2 - M_{W_L}^2)}. \tag{B14}$$

From Eq. (B14) and Eq. (B8), one readily verifies that the vertex function F_D is fairly insensitive to the quark mass. The absorptive parts of the $q^2 = M_H^2$ subtracted loop integrals are discarded. The dispersive component contributes to the on-shell mass renormalization of the Higgs field. We recall that the chosen subtraction identifies M_H with the one-loop pole mass.

Since the focus of the authors of Ref. [38] is the study of the cancelation of the gauge dependence their results are not inclusive of the interchange of W_L and W_R in the loops (the cancelation occurs independently in the two sectors). That amounts to an additional factor of 2 in Eq. (B6) and Eq. (B8) (the self-energy amplitude remains invariant). A different overall sign convention is also accounted for.

It is worth noting that in Eq. (B7) and Eq. (B8) only the terms that remain proportional to M_H^2 are relevant in the heavy H limit. On the other hand, perturbativity of the $H^0 G_L^+ G_R^-$ coupling ($G_{L,R}$ are the would-be Goldstone fields) bounds from above the scalar mass and it conservatively requires $M_H < 8 M_{W_R}$.

[1] J. C. Pati and A. Salam, Phys. Rev. D **10**, 275 (1974); J. C. Pati and A. Salam, Phys. Rev. D **11**, 703(E) (1975)].
[2] R. N. Mohapatra and J. C. Pati, Phys. Rev. D **11**, 566 (1975).
[3] R. N. Mohapatra and J. C. Pati, Phys. Rev. D **11**, 2558 (1975).
[4] G. Senjanović and R. N. Mohapatra, Phys. Rev. D **12**, 1502 (1975).
[5] G. Senjanović, Nucl. Phys. **B153**, 334 (1979).
[6] P. Minkowski, Phys. Lett. B **67**, 421 (1977).
[7] M. Gell-Mann, P. Ramond, and R. Slansky, in *Supergravity*, edited by P. van Nieuwenhuizen and D. Z. Freedman (North- Holland, Amsterdam, 1979), p. 315.
[8] T. Yanagida, in *Proceedings of Workshop on the Baryon Number of the Universe and Unified Theories, Tsukuba, Japan, 1979*, edited by O. Sawada and A. Sugamoto, p. 95.
[9] S. L. Glashow, in *Proceedings of Cargese 1979 Quarks and Leptons* edited by G. 't Hooft *et al.*, (Plenum Press, New York, 1980) p. 438; (NATO Adv. Study Inst. Ser. B Phys. **59** (1980) 687).
[10] R. N. Mohapatra and G. Senjanović, Phys. Rev. Lett. **44**, 912 (1980).
[11] G. Feinberg, M. Goldhaber, and G. Steigman, Phys. Rev. D **18**, 1602 (1978).
[12] R. N. Mohapatra and G. Senjanovic, Phys. Rev. D **23**, 165 (1981).
[13] V. Tello, M. Nemevsek, F. Nesti, G. Senjanovic, and F. Vissani, Phys. Rev. Lett. **106**, 151801 (2011).
[14] S. Hannestad, A. Mirizzi, G. G. Raffelt, and Y. Y. Y. Wong, J. Cosmol. Astropart. Phys. 08 (2010) 001.
[15] M. Archidiacono, S. Hannestad, A. Mirizzi, G. Raffelt, and Y. Y. Y. Wong, J. Cosmol. Astropart. Phys. 10 (2013) 020.
[16] W.-Y. Keung and G. Senjanovic, Phys. Rev. Lett. **50**, 1427 (1983).
[17] M. Nemevsek, G. Senjanovic, and Y. Zhang, J. Cosmol. Astropart. Phys. 07 (2012) 006.
[18] M. Nemevsek, F. Nesti, G. Senjanovic, and V. Tello, arXiv:1112.3061.
[19] M. Nemevsek, G. Senjanovic, and V. Tello, Phys. Rev. Lett. **110**, 151802 (2013).
[20] Y. Zhang, H. An, X. Ji, and R. N. Mohapatra, Nucl. Phys. **B802**, 247 (2008).
[21] A. Maiezza, M. Nemevšek, F. Nesti, and G. Senjanović, Phys. Rev. D **82**, 055022 (2010).
[22] D. Guadagnoli and R. N. Mohapatra, Phys. Lett. B **694**, 386 (2011).
[23] M. Blanke, A. J. Buras, K. Gemmler, and T. Heidsieck, J. High Energy Phys. 03 (2012) 024.
[24] J. Barry, L. Dorame, and W. Rodejohann, Eur. Phys. J. C **72**, 2023 (2012).
[25] J. A. Aguilar-Saavedra, F. Deppisch, O. Kittel, and J. W. F. Valle, Phys. Rev. D **85**, 091301 (2012).
[26] S. P. Das, F. F. Deppisch, O. Kittel, and J. W. F. Valle, Phys. Rev. D **86**, 055006 (2012).
[27] S. Bertolini, J. O. Eeg, A. Maiezza, and F. Nesti, Phys. Rev. D **86**, 095013 (2012).
[28] N. V. Krasnikov and V. A. Matveev, JETP Lett. **98**, 48 (2013) [Pis'ma Zh. Eksp. Teor. Fiz.**98**, 53 (2013)].
[29] T. Han, I. Lewis, R. Ruiz, and Z.-g. Si, Phys. Rev. D **87**, 035011 (2013); **87**, 039906(E) (2013).
[30] J. Barry and W. Rodejohann, J. High Energy Phys. 09 (2013) 153.
[31] E. Kou, C.-D. Lü, and F.-S. Yu, J. High Energy Phys. 12 (2013) 102.
[32] S. Bertolini, A. Maiezza, and F. Nesti, Phys. Rev. D **88**, 034014 (2013).
[33] P. S. B. Dev and R. N. Mohapatra, arXiv:1308.2151.
[34] P. S. B. Dev, C.-H. Lee, and R. N. Mohapatra, Phys. Rev. D **88**, 093010 (2013).
[35] W.-C. Huang and J. Lopez-Pavon, arXiv:1310.0265.
[36] A. Roitgrund, G. Eilam, and S. Bar-Shalom, arXiv:1401.3345.
[37] D. Chang, J. Basecq, L.-F. Li, and P. B. Pal, Phys. Rev. D **30**, 1601 (1984).
[38] J. Basecq, L.-F. Li, and P. B. Pal, Phys. Rev. D **32**, 175 (1985).
[39] W.-S. Hou and A. Soni, Phys. Rev. D **32** (1985) 163.
[40] G. Ecker and W. Grimus, Nucl. Phys. **B258**, 328 (1985).

[41] D. Chang, R. N. Mohapatra, and M. K. Parida, Phys. Rev. Lett. **52**, 1072 (1984).
[42] D. Chang, R. N. Mohapatra, and M. K. Parida, Phys. Rev. D **30**, 1052 (1984).
[43] G. Senjanović, Riv. Nuovo Cimento **034**, 1 (2011).
[44] C. Arbelaez, M. Hirsch, M. Malinsky, and J. C. Romao, arXiv:1311.3228.
[45] G. Senjanovic and P. Senjanovic, Phys. Rev. D **21**, 3253 (1980).
[46] M. Nemevsek, F. Nesti, G. Senjanovic, and Y. Zhang, Phys. Rev. D **83**, 115014 (2011).
[47] J. M. Frere, J. Galand, A. Le Yaouanc, L. Oliver, O. Pene, and J. C. Raynal, Phys. Rev. D **46**, 337 (1992).
[48] A. J. Buras, S. Jager, and J. Urban, Nucl. Phys. **B605**, 600 (2001).
[49] M. I. Vysotsky, Yad. Fiz. **31**, 1535 (1980) [Sov. J. Nucl. Phys. **31**, 797 (1980)].
[50] P. A. Boyle, N. Garron, and R. J. Hudspith (RBC and UKQCD Collaborations), Phys. Rev. D **86**, 054028 (2012).
[51] V. Bertone *et al.* (ETM Collaboration), J. High Energy Phys. 03 (2013) 089; ,07 (2013) 143(E).
[52] T. Bae *et al.* (SWME Collaboration), Phys. Rev. D **88** (2013) 071503.
[53] A. T. Lytle, P. A. Boyle, N. Garron, R. J. Hudspith, C. T. Sachrajda (RBC-UKQCD Collaboration) arXiv:1311.0322.
[54] S. Aoki *et al.*, arXiv:1310.8555.
[55] J. P. Silva and L. Wolfenstein, Phys. Rev. D **55**, 5331 (1997).
[56] Y. Grossman, Y. Nir, and M. P. Worah, Phys. Lett. B **407**, 307 (1997).
[57] N. G. Deshpande, B. Dutta, and S. Oh, Phys. Rev. Lett. **77**, 4499 (1996).
[58] A. Lenz and U. Nierste, J. High Energy Phys. 06 (2007) 072.
[59] J. Charles, A. Höcker, H. Lacker, S. Laplace, F. R. Diberder, J. Malclés, J. Ocariz, M. Pivk, and L. Roos (CKMfitter Group), Eur. Phys. J. C **41**, 1 (2005), updated results and plots available at http://ckmfitter.in2p3.fr.
[60] A. J. Buras and J. Girrbach, arXiv:1306.3775.
[61] S. Herrlich and U. Nierste, Nucl. Phys. **B419**, 292 (1994).
[62] S. Herrlich and U. Nierste, Nucl. Phys. **B476**, 27 (1996).
[63] J. Brod and M. Gorbahn, Phys. Rev. D **82**, 094026 (2010).
[64] J. Brod and M. Gorbahn, Phys. Rev. Lett. **108**, 121801 (2012).
[65] A. J. Buras, J.-M. Gerard, and W. A. Bardeen arXiv:1401.1385.
[66] A. J. Buras, D. Guadagnoli, and G. Isidori, Phys. Lett. B **688**, 309 (2010).
[67] V. Antonelli, S. Bertolini, M. Fabbrichesi, and E. I. Lashin, Nucl. Phys. **B493**, 281 (1997).
[68] S. Bertolini, J. O. Eeg, M. Fabbrichesi and E. I. Lashin, Nucl. Phys. **B514**, 63 (1998).
[69] N. H. Christ, T. Izubuchi, C. T. Sachrajda, A. Soni and J. Yu, Phys. Rev. D **88**, 014508 (2013).
[70] J. Yu, *Proc. Sci.*, LATTICE (**2013**) 398.
[71] A. Ferrari, J. Collot, M-L. Andrieux, B. Belhorma, P. de Saintignon, J-Y. Hostachy, Ph. Martin, and M. Wielers, Phys. Rev. D **62** (2000) 013001.
[72] S. N. Gninenko, M. M. Kirsanov, N. V. Krasnikov, and V. A. Matveev, Phys. At. Nucl. **70**, 441 (2007).
[73] M. Nemevšek, G. Senjanović, and V. Tello (to be published).
[74] G. Aad *et al.* (ATLAS Collaboration), Eur. Phys. J. C **72**, 2056 (2012).
[75] CMS Collaboration (CMS Collaboration for the collaboration), CMS-PAS-EXO-12-017.
[76] S. Chatrchyan *et al.* (CMS Collaboration) arXiv:1402.2176.
[77] J. Charles, S. Descotes-Genon, Z. Ligeti, S. Monteil, M. Papucci, and K. Trabelsi arXiv:1309.2293.
[78] A. Maiezza and M. Nemevšek (to be published).
[79] G. Senjanovic and J. C. Vasquez (to be published).
[80] T. Inami and C. S. Lim, Prog. Theor. Phys. **65**, 297 (1981); **65**, 1772(E) (1981).